$\mathcal{R}$esearch in
$\mathcal{A}$stronomy and
$\mathcal{A}$strophysics

New photometric studies for two deep, low-mass ratio overcontact binaries: Y Sex and V1363 Ori

Yuan-Gui Yang⋆, Shuang Wang, Hui-Yu Yuan and Hai-Geng Dai

School of Physics and Electronic Information, Huaibei Normal University, Huaibei 235000, China; *yygcn@163.com*

Abstract We present new photometry for two contact binaries, Y Sex and V1363 Ori, which were observed by three small telescopes in China. By using the W-D method, the absolute parameters are updated from new *BVR* light curves and previous radial velocity curves. Results identify that two binaries are deep, low-mass ratio (DLMR) overcontact binaries with $q \leq 0.25$ and $f \geq 50\%$. From the temperature-luminosity diagram, the primary components are slightly evolved main-sequence stars, whose evolutionary ages are $\sim 2.51\,\mathrm{Gyr}$ for Y Sex and $\sim 3.56\,\mathrm{Gyr}$ for V 1363 Ori, respectively. From the $(O - C)$ curves, it is found that the orbital periods may be undergoing secular increase with cyclic variations, which may be interpreted either by magnetic activity cycles or by the light-time orbit effect. With period increasing, this kind of DLMR overcontact binaries, such as Y Sex and V1363 Ori, will evolve into the rapid-rotating single stars.

Key words: binaries (including multiple): close — binaries: eclipsing — stars: fundamental parameters — stars: individual (Y Sex, V1363 Ori)

1 INTRODUCTION

W UMa-type binaries are the most frequently observed type of eclipsing binary systems owing to their relatively short orbital periods, generally ranging from 0.2 to 1.5 days (Geske et al. 2006). Contact binaries are an excellent source of accurate stellar parameters (e.g., mass, radius, and luminosity), which are deduced from light curves (LCs) and radial velocity (RV) curves using photometry and spectroscopy. Theoretical studies have suggested that contact binaries may undergo a periodic thermal-relaxation oscillation (Flannery 1976; Robertson & Eggleton 1977), and there have recently been many reviews of such objects (Van Hamme & Cohen 2008; Webbink 2003). Torres et al. (2010) listed 95 detached binaries with the known mass and radius of both stars having errors in accuracy of $\pm 3\%$ or better, with only 26 (or $\sim 14\%$) having a mass greater than $3\,M_\odot$. Several studies indicate that three evolutionary routes of case A binary can evolve low-mass detached binaries into contact ones (Eggleton 2006; Nelson & Eggleton 2001; Eggleton 2000). Recently, Jiang (2020) suggested that the low-mass contact binaries are formed during the thermal/nuclear-time-scale mass transfer phase, whereas a binary merger event can occur during the dynamical-time-scale mass transfer phase. Some investigators have

recently derived certain empirical relationships between correlating physical parameters from different samples of known contact binaries (Csizmadia & Klagyivik 2004; Latković et al. 2021; Gazeas et al. 2021; Qian et al. 2020; Zhang & Qian 2020; Sun et al. 2020). Zhang et al. (2020) suggested that an over-luminosity of a less massive component may be attributed to the energy transfer of a W-type contact binary or an initially more massive star of an A-type binary. Late-type contact binaries may provide an excellent opportunity to study stellar merging scenarios (Webbink 1976; Stępień 2006), which was identified by the merging event of V1309 Sco (Tylenda et al. 2011) and a merger candidate ZZ PsA (Wadhwa et al. 2021). Owing to some unsolved problems, such as the formation mechanism of young W UMa binaries (Jiang et al. 2014), the contact binaries are still of significant interest. Based on 46 deep, low-mass ratio (DLMR) overcontact binaries ($q \leq 0.25$ and $f \geq 50\%$), Yang & Qian (2015) suggested that they may merge into a rapid-rotating single star only if its mass ratio is approximately $0.044(\pm 0.007)$. In order to continuously observe this kind of sample binaries, Y Sex and V1363 Ori are chosen to investigate their physical properties.

Y Sex (BD+01°2394 = HD 87079, $V = 9^{\mathrm{m}}95$) is a contact binary within a tight visual double star (EAS 1997). Its light variability was first noted by (Hoffmeister 1934). The spectral type of this binary is

---

⋆ Corresponding author

F5/6. Owing to its short period (∼0.4198 days) and proper magnitude, this eclipsing binary was observed and studied by several investigators. McLean & Hilditch (1983) obtained spectroscopic observations and derived a mass ratio of 0.18(±0.03). However, Pribulla et al. (2009) updated it to $q_{sp} = 0.195(\pm0.008)$ based on their radial velocity data. They estimated the light contribution of the visual companion for the central binary up to 11(±3)%. In addition, Tanabe & Nakamura (1957), Yang & Liu (2003), and Gazeas et al. (2021) performed photoelectric/CCD photometry for this binary, and several investigators have analyzed its period variations based on different databases, and gave the different results. It is therefore necessary to reanalyze its period changes.

V1363 Ori (BD-00°845 = HD 289949) was first noted using the *Hipparcos* satellite. It was classified as an EW-type binary with a period of $0^d431915$, and was updated to $0^d4319281$ (Kreiner 2004). In addition, the visual brightness varies from 10^m346 to 10^m590. Moreover, Nesterov et al. (1995) derived a spectral type of F5 from Henry Draper Extension Charts, whereas for technical reasons Pych et al. (2004) confined it to the early to mid-F. From the LAMOST survey database[1], a low-resolution spectrum was obtained on 2012 December 24. Its spectral type and temperature were determined to be F6 and 6156(±76) K, respectively. In addition, Selam (2004) derived a photometric solution from the *Hipparcos* data. Gazeas & Niarchos (2005) also observed this star and obtained a spotted solution from the normal light curves, which seemly identified the existence of the O'Connell effect (Gomez-Forrellad et al. 1999). Moreover, Pych et al. (2004) published 38 radial velocities and derived a mass ratio of $q_{sp} = 0.205(\pm0.015)$, and Gazeas et al. (2021) recently determined its absolute parameters from Pych et al. (2004)'s radial velocities and the *BVRI*-band light curves in 2003.

The present paper is organized as follows. We photometrically observed two contact binaries Y Sex and V1363 Ori, in Section 2. Together with new light minimum times, the orbital period changes were analyzed in Section 3. Then we deduced the photometric-spectroscopic solutions from RV curves and LCs by the W-D method in Section 4. Finally, the absolute parameters for two binaries were updated, and we gave some discussions on period variations and their possible evolutionary scenarios.

2 NEW PHOTOMETRY AND DATA REDUCTION AT XINGLONG STATION

New light curves of Y Sex and V1363 Ori were conducted on six nights in 2021 by using the 60-cm telescope (Li et al. 2009) at the Xinglong station (XLs) of National Astronomical Observatories, Chinese Academy of Sciences (NAOC). It has a focal ratio of $f/4.23$ with a CCD camera with a pixel resolution of 2048×2048. The standard Johnson-Cousins $UBVR_cI_c$ filters were equipped onto this telescope. All effective images for two binaries were reduced using the *IRAF*[2] in standard mode. The differential magnitudes (i.e., the variable *minus* comparison star) were then obtained using aperture photometry.

The detailed observational information of Y Sex and V1363 Ori is given in Table 1, including the dates of observation, comparison and check stars, exposure times, and standard derivations. All individual data for the two binaries are available upon request. The standard derivation is determined from the magnitudes of the comparison and check stars. The complete *BVR* light curves are shown in both panels of Figure 1, the phases of which are computed by the initial epoch time (i.e., the observed light minimum times) and the orbital periods determined by Kreiner (2004). From Figure 1(a), Y Sex is an A-subtype contact binary with a total eclipse around phase of 0.5, whose duration time is ∼ 35 minutes. As shown in Figure 1(b), V1363 Ori evidently processes symmetric light curves with a low variable amplitude (∼ 0^m2), which agrees the LCs in 2003 (Gazeas et al. 2021). However, Gomez-Forrellad et al. (1999) and Gazeas & Niarchos (2005) reported the existence of O'Connell effect for this binary. Therefore, the intrinsic light variability occurs in this binary, which is similar to the previously studied binaries, such as DZ Psc (Yang et al. 2013) and DF CVn (Dai et al. 2011).

3 ANALYZING ORBITAL PERIOD CHANGES

As shown in Figure 2, three eclipsing times for Y Sex and V1363 Ori were monitored, which are observed by the 60-cm telescope at the XLs and the 1.0-m telescope (Gu 1998) at Yunnan astronomical observatory (YNAO). From our new data, several eclipsing timings were determined using the K-W method (Kwee & van Woerden 1956). Table 2 lists those individual single-band times along with their standard derivations. Together with our new data, we compiled all available times of the minimum light to study their orbital period changes. During the computing process, the weights for individual eclipsing times are inversely proportional to the squared standard derivations whether if they are observed or suggested.

3.1 Y Sex

Several investigators have proposed the period variations to a secular decrease (Herczeg 1993), light-time effect

---

Table 1 Observed Information for Light Curves

Variable Star	Y Sex	V1363 Ori
Observing dates	2021 Jan 12 & 13	2021 Jan 29, 30, 31 & Feb 1
Comparison star	TYC 244-1170-1	BD 00 833
Check star	HD 86901	HD 289951
Exposure times	40s(B), 30s(V) & 20s(R_c)	50s(B), 30s(V) & 20s(R_c)
Number of data	316(B), 317(V) & 315(R_c)	523(B), 535(V) & 527(R_c)
Standard derviation ($\times 10^{-3}$)	$\pm 7^m 8(B)$, $\pm 5^m 7(V)$, $\pm 5^m 0(R)$	$\pm 7^m 6(B)$, $\pm 4^m 9(V)$, $\pm 5^m 4(R)$
Variable amplitude	$0^m 41(B)$, $0^m 39(V)$, $0^m 38(R)$	$0^m 24(B)$, $0^m 22(V)$, $0^m 22(R)$
[a] Initial epoch time	HJD 2459227.3138	HJD 2459244.1341
[b] Orbital period (d)	0.4198193	0.4319281

Notes: [a] The adopted initial epoch times are the observed primary times of minimum light; [b] The orbital periods are taken from Kreiner (2004).
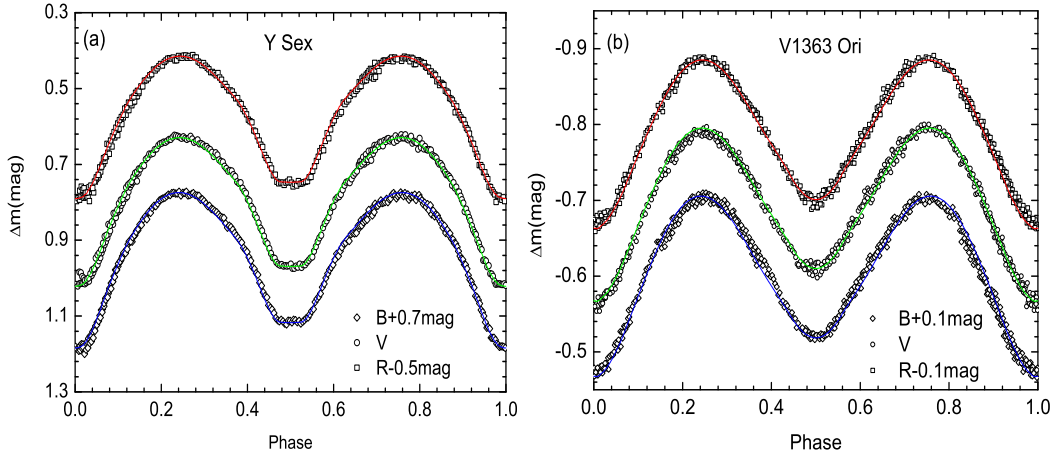

Fig. 1 *BVR*-band LCs for Y Sex (a) and V1363 (b) during the 2020–2021 observing season. Theoretical LCs as color lines are computed from the solutions from Table 6.

Table 2 New Light Minimum Times for Y Sex and V1363 Ori

Star	JD(Hel.)	Error	Min	Band	Telescope
Y Sex	2459227.31348	± 0.00014	I	B	60-cm
	2459227.31383	± 0.00012	I	V	60-cm
	2459227.31401	± 0.00017	I	R	60-cm
	2459228.36347	± 0.00017	II	B	60-cm
	2459228.36351	± 0.00016	II	V	60-cm
	2459228.36382	± 0.00022	II	R	60-cm
	2459243.26660	± 0.00019	I	B	80-cm
	2459243.26674	± 0.00014	I	V	80-cm
	2459243.26696	± 0.00015	I	R	80-cm
	2459313.16846	± 0.00075	II	V	60-cm
	2459313.16766	± 0.00057	II	R	60-cm
V1363 Ori	2458871.16872	± 0.00035	II	B	1.0-m
	2458871.16798	± 0.00032	II	V	1.0-m
	2458871.16894	± 0.00034	II	R	1.0-m
	2458872.03036	± 0.00038	II	B	1.0-m
	2458872.02981	± 0.00035	II	V	1.0-m
	2458872.02939	± 0.00049	II	R	1.0-m
	2458902.04934	± 0.00023	II	B	60-cm
	2458902.05113	± 0.00020	II	V	60-cm
	2458902.05119	± 0.00023	II	R	60-cm
	2459244.13346	± 0.00078	I	B	60-cm
	2459244.13431	± 0.00044	I	V	60-cm
	2459244.13443	± 0.00037	I	R	60-cm
	2459244.99686	± 0.00020	I	R	60-cm
	2459244.99733	± 0.00024	I	R	60-cm
	2459244.99732	± 0.00021	I	R	60-cm
	2459246.07721	± 0.00034	II	R	60-cm
	2459246.07638	± 0.00036	II	R	60-cm
	2459246.07651	± 0.00039	II	R	60-cm

(Wolf et al. 2000), abrupt or cyclic variation (Qian & Liu 2000), or two cyclic oscillations (He & Qian 2007), which may result from the incomplete database sets of the eclipsing times. Therefore, we collected all available times of minimum light, including 20 photographic, four visual, 53 photoelectric, and 81 CCD measurements, which are listed in Table 3. Several comments are listed as follows: (1) four light minimum times along with their errors were re-determined from the *UBV* observations of Hill (1979); (2) the derivations for other two eclipsing times (Yang & Liu 2003) are computed from their *V*-band observations; (3) the errors are assumed to be 0.001 days for "pg" and "vi" data; (4) the standard derivations for "pe" and CCD data are averaged to an error of 0.0006 days, which is accepted for this type of data without uncertainties[3].

For all 158 light minimum times of Y Sex, the initial residuals are computed by using the linear ephemeris (Hill 1979),

$$\text{Min.I} = \text{HJD } 2439521.964(\pm 0.003) \\ + 0.41981543(\pm 0.00000004) \times E. \quad (1)$$

---

[3] Most "pe" data are from *BAV* (https://www.bav-astro.eu/), whereas all 25 CCD measurements are from *Variable Star Bulletin of Japan* (http://vsolj.cetus-net.org/).
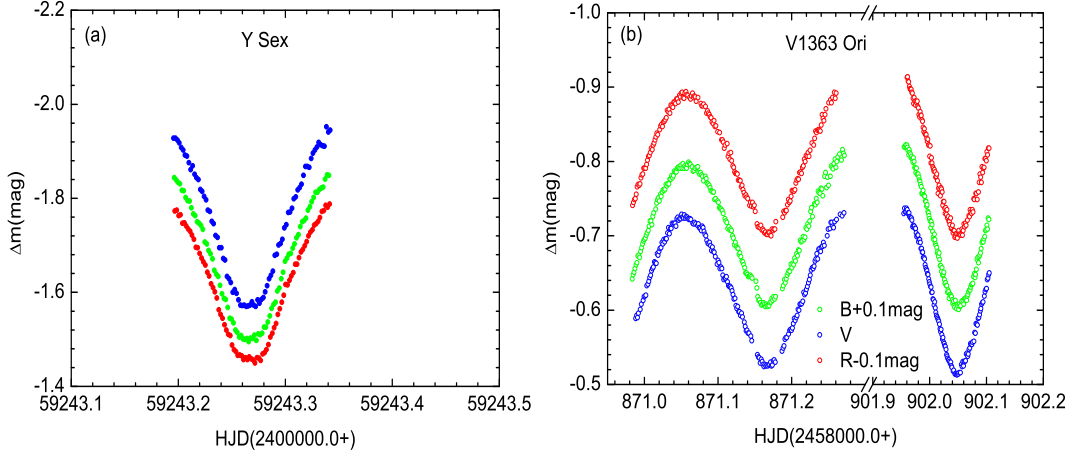
Fig. 2 Eclipsing times observed for (a) Y Sex on 2021 Jan 29, and (b) V1363 Ori on 2020 Jan 22 using the 60-cm telescope and on 2020 Feb 22 using the 1.0-m telescope at YNAO.
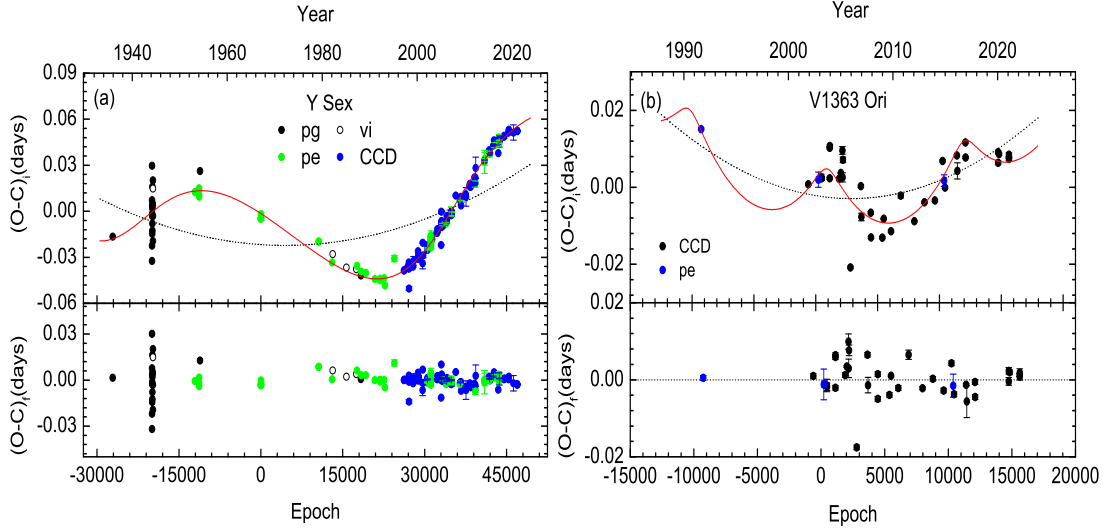

Fig. 3 Residuals of $(O - C)$ for Y Sex (a) and V1363 Ori (b). The *filled blue* and *black circles* are photometric and CCD measurements, while the *open circles* represent visual measurements. The *solid* and *dotted lines* are plotted by Eq. (2) and its parabolic part, respectively.

Residuals of $(O - C)_i$ are tabulated in Table 3 and shown in the upper panel of Figure 3(a). From this figure, the $(O - C)_i$ curve displays a large oscillation and its general trend is upward. The initial residuals are then fitted by the light-time orbit effect with an upward parabola, i.e.,

$$(O - C)_i = \Delta T + \Delta P \times E + Q \times E^2$$
$$+ \frac{a_{12} \sin i}{c} \left[\frac{1 - e^2}{1 + e \cos \nu} + e \sin \omega \right], \quad (2)$$

where T and Q are the initial epoch time and the variation in the period rate. The last term of Equation (2) is the light-time orbit effect (Irwin 1952), in which a_{12}, e, i, ω, and ν are the orbital parameters for the eclipsing pair around the mass center of the binary system. Adopting the non-linear least-squares method (Yang 2009), we simultaneously derived seven fitting parameters with their

standard derivations, which are given in Table 4. With the help of Equation (2), we obtained the final residuals, listed in Table 3. The corresponding $(O - C)_f$ curve is shown in the lower panel of Figure 4. Although some large scatter still exists for "pg" data, the general trend of $(O - C)_i$ is well fitted. No regularities exist in the $(O - C)_f$ diagram. The orbital period increases at a rate of $4.58(\pm0.35)$ d yr^{-1}. The modulated period of $P_{mod} = 65.2(\pm0.7)$ yr is larger than the previous values of 51.2 yr (He & Qian 2007) and 57.6 yr (Wolf et al. 2000), which result from the incomplete database of light minimum times.

3.2 V1363 Ori

We accumulated 39 light minimum times along with new data, as listed in Table 5. From this table, the uncertainties

Table 3 All Compiled Light Minimum Times of Y Sex

JD(Hel.)	Error (d)	Epoch	Method	Min	$(O-C)_i$ (d)	$(O-C)_f$ (d)	Ref.
2428122.700		−27153.0	pg	I	−0.0165	+0.0019	[1]
2431150.455		−19941.0	pg	I	+0.0296	+0.0303	[1]
2431156.310		−19927.0	pg	I	+0.0072	+0.0079	[1]
2431157.120		−19925.0	pg	I	−0.0224	−0.0218	[1]
2431157.320		−19924.5	pg	II	−0.0323	−0.0317	[1]
2431162.387		−19912.5	pg	II	−0.0031	−0.0025	[1]
2431163.215		−19910.5	pg	II	−0.0147	−0.0141	[1]
2431170.160		−19894.0	pg	I	+0.0033	+0.0039	[1]
2431170.365		−19893.5	pg	II	−0.0016	−0.0010	[1]
2431176.260		−19879.5	pg	II	+0.0160	+0.0165	[1]
2431178.135		−19875.0	pg	I	+0.0018	+0.0023	[1]
2431178.335		−19874.5	pg	II	−0.0081	−0.0076	[1]
2431179.170		−19872.5	pg	II	−0.0127	−0.0122	[1]
2431197.240		−19829.5	pg	II	+0.0052	+0.0056	[1]
2431206.265		−19808.0	pg	I	+0.0042	+0.0045	[1]
2431215.307		−19786.5	pg	II	+0.0202	+0.0204	[1]
2431216.317		−19784.0	pg	I	−0.0194	−0.0191	[1]
2431219.272		−19777.0	pg	I	−0.0031	−0.0029	[1]
2431219.290		−19777.0	vi	I	+0.0149	+0.0151	[2]
2434445.989		−12091.0	pe	I	+0.0125	−0.0007	[3]
2434770.089		−11319.0	pe	I	+0.0150	+0.0015	[3]
2434771.1330		−11316.5	pe	II	+0.0095	−0.0040	[4]
2434771.135		−11316.5	pe	II	+0.0115	−0.0020	[5]
2434838.74		−11155.5	pg	II	+0.0262	+0.0127	[6]
2439521.9603	±0.0004	+0.0	pe	I	−0.0045	−0.0033	[7]
2439528.8868	±0.0009	16.5	pe	II	−0.0050	−0.0037	[7]
2439529.9370	±0.0003	19.0	pe	I	−0.0043	−0.0030	[7]
2439539.8052	±0.0011	42.5	pe	II	−0.0018	−0.0004	[7]
2443965.6915		10585.0	pe	I	−0.0197	+0.0088	[8]
2443973.6678		10604.0	pe	I	−0.0199	+0.0086	[8]
2445001.3624	±0.0002	13052.0	pe	I	−0.0334	+0.0007	[9]
2445044.3990		13154.5	vi	II	−0.0279	+0.0065	[10]
2446095.6080		15658.5	vi	II	−0.0367	+0.0025	[11]
2446862.4000		17485.0	vi	I	−0.0376	+0.0043	[12]
2446909.4215		17597.0	pe	I	−0.0355	+0.0066	[13]
2447214.4110		18323.5	pg	II	−0.0419	+0.0010	[12]
2447239.3926		18383.0	pe	I	−0.0393	+0.0036	[12]
2447592.4566		19224.0	pe	I	−0.0401	+0.0036	[14]
2448279.4805		20860.5	pe	II	−0.0441	+0.0002	[15]
2448691.3186		21841.5	pe	II	−0.0450	−0.0006	[16]
2448691.5296		21842.0	pe	I	−0.0439	+0.0004	[16]
2449005.5518		22590.0	pe	I	−0.0436	+0.0004	[17]
2449057.3942		22713.5	pe	II	−0.0484	−0.0045	[17]
2449789.3600	±0.0020	24457.0	pe	I	−0.0308	+0.0114	[18]
2450519.621		26196.5	CCD	II	−0.0388	+0.0001	[19]
2450548.3789	±0.0004	26265.0	CCD	I	−0.0382	+0.0005	[20]
2450823.5701	±0.0002	26920.5	CCD	II	−0.0360	+0.0010	[21]
2450897.4562	±0.0007	27096.5	CCD	II	−0.0374	−0.0009	[22]
2450904.3837	±0.0004	27113.0	CCD	I	−0.0369	−0.0004	[22]
2450907.9557	±0.0006	27121.5	CCD	II	−0.0333	+0.0031	[23]
2450914.0260	±0.0012	27136.0	CCD	I	−0.0503	−0.0140	[23]
2451233.1000	±0.0004	27896.0	CCD	I	−0.0361	−0.0020	[23]
2451268.9980	±0.0028	27981.5	CCD	II	−0.0323	+0.0015	[23]
2451600.4438	±0.0007	28771.0	CCD	I	−0.0308	+0.0002	[24]
2451608.635		28790.5	CCD	II	−0.0260	+0.0049	[19]
2451617.0271		28810.5	CCD	II	−0.0302	+0.0006	[25]
2451618.0757		28813.0	CCD	I	−0.0311	−0.0003	[25]
2451655.4420	±0.0005	28902.0	CCD	I	−0.0284	+0.0021	[26]
2451663.4184	±0.0001	28921.0	CCD	I	−0.0285	+0.0019	[26]
2451965.4701	±0.0036	29640.5	CCD	II	−0.0340	−0.0065	[27]
2451971.3610	±0.0005	29654.5	CCD	II	−0.0205	+0.0069	[24]
2452001.3695	±0.0014	29726.0	CCD	I	−0.0288	−0.0017	[28]
2452325.0538		30497.0	CCD	I	−0.0222	+0.0014	[29]
2452326.1004		30499.5	CCD	II	−0.0251	−0.0015	[29]
2452341.4258	±0.0004	30536.0	CCD	I	−0.0230	+0.0005	[30]
2452352.1290	±0.0002	30561.5	pe	II	−0.0251	−0.0018	[31]

Table 3 *Continued.*

JD(Hel.)	Error (d)	Epoch	Method	Min	$(O-C)_i$ (d)	$(O-C)_f$ (d)	Ref.
2452353.1798	±0.0003	30564.0	pe	I	−0.0239	−0.0005	[31]
2452598.9880	±0.0010	31149.5	pe	II	−0.0176	+0.0029	[32]
2452600.0360	±0.0010	31152.0	pe	I	−0.0191	+0.0014	[32]
2452600.2478	±0.0008	31152.5	pe	II	−0.0172	+0.0033	[32]
2452600.4547	±0.0009	31153.0	pe	I	−0.0202	+0.0003	[32]
2452600.6650	±0.0020	31153.5	pe	II	−0.0198	+0.0006	[32]
2452600.8759	±0.0005	31154.0	pe	I	−0.0188	+0.0016	[32]
2452601.0844	±0.0007	31154.5	pe	II	−0.0203	+0.0002	[32]
2452601.2982	±0.0004	31155.0	pe	I	−0.0164	+0.0041	[32]
2452602.1320	±0.0006	31157.0	pe	I	−0.0222	−0.0017	[32]
2452602.3443	±0.0008	31157.5	pe	II	−0.0198	+0.0007	[32]
2452602.9703	±0.0008	31159.0	pe	I	−0.0235	−0.0031	[32]
2452603.1880	±0.0030	31159.5	pe	II	−0.0157	+0.0047	[32]
2452603.3950	±0.0007	31160.0	pe	I	−0.0186	+0.0018	[32]
2452603.6037	±0.0006	31160.5	pe	II	−0.0199	+0.0006	[32]
2452603.8143	±0.0004	31161.0	pe	I	−0.0192	+0.0013	[32]
2452604.0249	±0.0006	31161.5	pe	II	−0.0185	+0.0020	[32]
2452698.0639		31385.5	CCD	II	−0.0181	+0.0012	[33]
2453046.0950		32214.5	CCD	II	−0.0140	+0.0010	[33]
2453078.2108	±0.0003	32291.0	CCD	I	−0.0141	+0.0005	[34]
2453091.2258	±0.0001	32322.0	CCD	I	−0.0134	+0.0011	[35]
2453094.3761	±0.0005	32329.5	CCD	II	−0.0117	+0.0027	[36]
2453386.5573	±0.0004	33025.5	CCD	II	−0.0220	−0.0115	[37]
2453400.4330	±0.0004	33058.5	CCD	II	−0.0002	+0.0101	[37]
2453410.7111	±0.0009	33083.0	CCD	I	−0.0076	+0.0026	[38]
2453411.7596	±0.0014	33085.0	CCD	II	−0.0086	+0.0016	[38]
2453412.8075	±0.0010	33088.0	CCD	I	−0.0103	−0.0001	[38]
2453413.6501	±0.0011	33090.0	CCD	I	−0.0073	+0.0029	[38]
2453424.1465		33115.0	CCD	I	−0.0063	+0.0038	[39]
2453464.4464	±0.0008	33211.0	pe	I	−0.0087	+0.0008	[40]
2453498.6604	±0.0013	33292.5	CCD	II	−0.0097	−0.0006	[41]
2453769.4430	±0.0005	33937.5	pe	II	−0.0080	−0.0026	[42]
2453812.0566		34039.0	CCD	I	−0.0057	−0.0009	[43]
2453816.0437		34048.5	CCD	II	−0.0068	−0.0021	[43]
2453818.3541	±0.0002	34054.0	CCD	I	−0.0054	−0.0007	[37]
2453836.1986	±0.0003	34096.5	CCD	II	−0.0031	+0.0014	[34]
2454133.2197		34804.0	CCD	I	−0.0014	−0.0010	[44]
2454144.1337		34830.0	CCD	I	−0.0026	−0.0024	[44]
2454164.2875	±0.0004	34878.0	CCD	I	+0.0001	+0.0000	[34]
2454168.0636		34887.0	CCD	I	−0.0022	−0.0023	[44]
2454171.0021		34894.0	CCD	I	−0.0024	−0.0026	[44]
2454173.3130	±0.0029	34899.5	pe	II	−0.0004	−0.0007	[42]
2454173.5234	±0.0029	34900.0	pe	I	+0.0001	−0.0002	[42]
2454191.3641	±0.0020	34942.5	CCD	II	−0.0014	−0.0019	[37]
2454213.4053	±0.0002	34995.0	pe	I	−0.0005	−0.0013	[45]
2454507.4968	±0.0004	35695.5	CCD	II	+0.0103	+0.0053	[45]
2454830.3323		36464.5	CCD	II	+0.0077	−0.0017	[46]
2454838.5180	±0.0002	36484.0	pe	I	+0.0070	−0.0025	[47]
2454862.8687	±0.0003	36542.0	CCD	I	+0.0084	−0.0015	[48]
2454907.9998		36649.5	CCD	II	+0.0094	−0.0012	[49]
2454919.9589		36678.0	CCD	I	+0.0037	−0.0070	[49]
2455244.4825	±0.0003	37451.0	CCD	I	+0.0100	−0.0051	[50]
2455265.4744	±0.0004	37501.0	CCD	I	+0.0111	−0.0043	[51]
2455298.8480	±0.0060	37580.5	CCD	II	+0.0094	−0.0065	[52]
2455579.9212	±0.0009	38250.0	CCD	I	+0.0162	−0.0034	[53]
2455596.0858		38288.5	CCD	II	+0.0179	−0.0019	[54]
2455597.1345		38291.0	CCD	I	+0.0170	−0.0028	[54]
2455631.9781		38374.0	CCD	I	+0.0159	−0.0043	[54]
2455648.3509	±0.0003	38413.0	CCD	I	+0.0159	−0.0046	[55]
2455668.7127	±0.0006	38461.5	CCD	II	+0.0167	−0.0041	[53]
2455952.9331	±0.0003	39138.5	CCD	II	+0.0221	−0.0023	[56]
2456000.9985		39253.0	CCD	I	+0.0186	−0.0064	[57]
2456009.3940	±0.0020	39273.0	pe	I	+0.0178	−0.0073	[58]
2456014.0161		39284.0	CCD	I	+0.0219	−0.0033	[57]
2456035.6430	±0.0070	39335.5	CCD	II	+0.0283	+0.0029	[56]
2456723.5145	±0.0076	40974.0	pe	I	+0.0322	−0.0013	[59]
2456726.0342		40980.0	CCD	I	+0.0330	−0.0005	[60]

Table 3 *Continued.*

JD(Hel.)	Error (d)	Epoch	Method	Min	$(O-C)_i$ (d)	$(O-C)_f$ (d)	Ref.
2456728.3443	±0.0041	40985.5	pe	II	+0.0342	+0.0006	[59]
2456728.5535	±0.0009	40986.0	pe	I	+0.0334	−0.0001	[59]
2457079.7354	±0.0002	41822.5	CCD	II	+0.0397	+0.0024	[61]
2457091.4879	±0.0018	41850.5	pe	II	+0.0374	−0.0001	[62]
2457106.3924	±0.0002	41886.0	CCD	I	+0.0385	+0.0008	[63]
2457145.0149		41978.0	CCD	I	+0.0379	−0.0001	[64]
2457396.6993	±0.0004	42577.5	CCD	II	+0.0430	+0.0024	[63]
2457450.0191		42704.5	CCD	II	+0.0462	+0.0051	[65]
2457474.3653	±0.0016	42762.5	pe	II	+0.0431	+0.0018	[66]
2457777.0470		43483.5	CCD	II	+0.0379	−0.0062	[67]
2457778.1041		43486.0	CCD	I	+0.0455	+0.0013	[67]
2457810.0113		43562.0	CCD	I	+0.0467	+0.0023	[67]
2457829.3243	±0.0020	43608.0	pe	I	+0.0482	+0.0036	[68]
2457829.5296	±0.0015	43608.5	pe	II	+0.0436	−0.0010	[68]
2457839.3970	±0.0011	43632.0	pe	I	+0.0453	+0.0006	[68]
2457860.5983	±0.0002	43682.5	CCD	II	+0.0459	+0.0011	[69]
2457865.4260	±0.0040	43694.0	CCD	I	+0.0458	+0.0008	[70]
2458218.7034	±0.0011	44535.5	CCD	II	+0.0485	+0.0006	[71]
2458234.6571	±0.0001	44573.5	CCD	II	+0.0492	+0.0012	[71]
2458565.4737	±0.0011	45361.5	CCD	II	+0.0512	+0.0006	[72]
2458598.6411	±0.0003	45440.5	CCD	II	+0.0532	+0.0024	[73]
2458949.3950	±0.0050	46276.0	CCD	I	+0.0513	−0.0020	[74]
2459227.3138	±0.0002	46938.0	CCD	I	+0.0523	−0.0028	[75]
2459228.3636	±0.0002	46940.5	CCD	II	+0.0526	−0.0026	[75]
2459243.2668	±0.0002	46976.0	CCD	I	+0.0523	−0.0029	[75]
2459313.1681	±0.0006	47142.5	CCD	II	+0.0544	−0.0013	[75]

References: [1] Prikhodjko (1947); [2] Zessewitsch (1947); [3] Tanabe & Nakamura (1957); [4] Huruhata (1958); [5] Szafraniec (1962); [6] Koch (1961); [7] Hill (1979); [8] Herczeg (1993); [9] Yang & Liu (1982); [10] Hübscher et al. (1994); [11] Hübscher et al. (1985); [12] Hübscher & Lichtenknecker (1988); [13] Braune & Hübscher (1987); [14] Hübscher et al. (1989); [15] Hübscher et al. (1991); [16] Hübscher et al. (1992); [17] Hübscher et al. (1993); [18] Diethelm (1998); [19] Samolyk (2012); [20] Agerer & Hübscher (1998a); [21] Agerer & Hübscher (1998b); [22] Agerer et al. (1999); [23] Nagai (2008a); [24] Agerer & Hübscher (2002); [25] Nagai (2001); [26] Wolf et al. (2000); [27] Zejda (2004); [28] Diethelm (2001); [29] Nagai (2003); [30] Šarounová & Wolf (2005); [31] Yang & Liu (2003); [32] Sobotka (2007); [33] Nagai (2004); [34] He & Qian (2007); [35] Krajci (2005); [36] Hübscher et al. (2005); [37] Brát et al. (2007); [38] Ogłoza et al. (2008); [39] Nagai (2006); [40] Hübscher et al. (2005); [41] Hübscher (2007); [42] Krajci (2006); [43] Nagai (2007); [44] Nagai (2008b); [45] Parimucha et al. (2009); [46] Nagai (2009); [47] Hübscher & Monninger (2011); [48] Diethelm (2009); [49] Nagai (2010); [50] Brát et al. (2011); [51] Parimucha et al. (2011); [52] Diethelm (2010); [53] Diethelm (2011); [54] Nagai (2012); [55] Parimucha et al. (2013); [56] Diethelm (2012); [57] Nagai (2014); [58] Hübscher (2013); [59] Hübscher & Lehmann (2015); [60] Nagai (2015); [61] Samolyk (2015); [62] Hübscher (2016); [63] Jurysek et al. (2017); [64] Nagai (2016); [65] Nagai (2017); [66] Hübscher (2017); [67] Nagai (2018); [68] Pagel (2018); [69] Samolyk (2017); [70] Paschke (2017); [71] Samolyk (2018); [72] Pagel (2020); [73] Samolyk (2019); [74] Paschke (2020); [75] Present paper.

of 17 data are not given in the literature. Similar to the same process applied for V1363 Ori, a mean error of $0^{\rm d}0004$ for 22 data is averaged as the assumed error for the light minimum time without the standard derivations.

From all light minimum times, we updated a new linear ephemeris as follows:

$$\text{Min.I} = \text{HJD } 2452500.0659(\pm 0.0019) \\ + 0.4319241(\pm 0.0000002) \times E. \quad (3)$$

Using Equation (3), we computed the initial residuals, which are listed in Table 5. The corresponding $(O-C)_i$ curve is displayed in the upper panel of Figure 3(b). From this figure, a long gap exists between HJD 2448500.0343 (*Hipparcos* epoch) and HJD 2452237.2413 (Kato & Takamizawa 2002). However, a cyclic variation is apparent, and the initial residuals are fitted using Equation (2). After some iterations, we obtained the fitted parameters of Equation (2), which are given in Table 4. The orbital period increases

at a rate of $1.56(\pm 0.06)$ d yr^{-1}. The modulated period is $P_{mod} = 13.4(\pm 0.3)$yr. The final residuals are listed in Table 5, and are shown in the lower panel of Figure 3(b). With the exception of HJD 2453708.1365 (Nagai 2006), the eclipsing data are fitted well. Its actual change still needs to be identified in future observations.

4 SPECTROSCOPIC-PHOTOMETRIC SOLUTIONS

Based on our new light curves and radial velocities (Pych et al. 2004; Pribulla et al. 2009), the modelled solutions were solved using the *W-D* method (Wilson & Devinney 1971; Wilson 2008; Wilson & Van Hamme 2014)[4]. This program is comprehensively applied in the modeling of binary stars, eclipses, and even intrinsic pulsations from their multiband

---

[4] Wilson-Devinney binary star modeling code (W-D program) may be available for downloading from the web site of `ftp://ftp.astro.ufl.edu/pub/wilson/lcdc2015`.

Table 4 Fitted and Deduced Parameters for Orbital Period Variations

Parameter	Y Sex	V1363 Ori
T (HJD)	2439521.9423(4)	2452500.0636(4)
P (d)	0.41981520(8)	0.43192400(8)
$Q(\times 10^{-11}$d$)$	$+2.63(\pm0.20)$	$+8.90(\pm0.50)$
A (d)	$0.0311(\pm0.0009)$	$0.0074(\pm0.0004)$
e	$0.224(\pm0.006)$	$0.564(\pm0.048)$
T_s (HJD)	2453562.7($\pm$247.2)	2448190.5($\pm$152.7)
ω (arc)	$6.023(\pm0.037)$	$1.608(\pm0.067)$
P_{mod} (yr)	$65.2(\pm0.7)$	$13.4(\pm0.3)$
$a_{12}\sin i$ (AU)	$5.38(\pm0.16)$	$1.28(\pm0.08)$
$\Delta P/P(\times 10^{-6})$	$8.21(\pm0.24)$	$9.53(\pm0.52)$
$f(m)$ $(\times 10^{-2} M_\odot)$	$3.97(\pm0.34)$	$1.17(\pm0.03)$
M_3 $(M_\odot)$	$0.62(\pm0.02)$	$0.41(\pm0.02)$
a_{12} (AU)	$15.9(\pm0.9)$	$4.41(\pm0.45)$
$^a D$ (pc)	$391.3(\pm45.5)$	$261.1(\pm22.3)$
$\alpha('')$	$0.025(\pm0.004)$	$0.059(\pm0.011)$
dP/dt $(\times 10^{-7}$d yr$^{-1})$	$0.46(\pm0.04)$	$1.56(\pm0.06)$
dm/dt $(\times 10^{-8} M_\odot$ yr$^{-1})$	$1.38(\pm0.10)$	$3.67(\pm0.15)$

Notes: ^{a}'D' refer to the distance away from the Sun, which is computed from the parallaxes (Gaia Collaboration et al. 2018).

data and radial velocities (Wilson et al. 2020a,b). During the modelling process, we adopted Model 3 (i.e., with an over-contact configuration). As usual, the gravity darken coefficients and bolometric albedo indexes are fixed to $g_{1,2} = 0.32$ and $A_{1,2} = 0.5$ (Lucy 1967; Rucinski 1973). Moreover, we applied the logarithmic limb-darkening coefficients (Van Hamme 1993).

4.1 Y Sex

For Y Sex, new *BVR$_c$* light curves are displayed in Figure 1(a), whereas the radial velocities are taken from (McLean & Hilditch 1983) and (Pribulla et al. 2009), as displayed in Figure 4(a). All observations were analyzed to deduce the photometric-spectroscopic solution. Based on the spectral type of F5/6 of Y Sex, we adopted a mean effective temperature of $T_p = 6400 \pm 100$ K (Gazeas et al. 2021). The mass ratio of $q_{sp} = 0.195$ (Pribulla et al. 2009) is assumed to be an input mass ratio. Meanwhile, the third light ℓ_3 as a free parameter is considered. After some iterations, we then obtained the orbital and geometric elements listed in Table 6. Theoretical LCs and RVs as solid lines are plotted in Figures 1(a) and 4(a), respectively. The final mass ratio is $q = 0.1954(\pm0.0009)$, which agrees with the spectroscopic mass ratio. The third light contributes to the luminosity of the binary system very low (i.e., $\sim 0.6\%$), which largely differs from the previous value of $\sim 11\%$ (Pribulla et al. 2009).

4.2 V1363 Ori

From the *LAMOST* survey database, the spectral type for V1363 Ori is F6, which is slightly later than F5 (Nesterov et al. 1995). We fixed the mean effective temperature of $T_p = 6156(\pm75)$ K, which is smaller

than the adopted value of 6750 K (Gazeas & Niarchos 2005) or 6700 K (Gazeas et al. 2021). As shown in Figure 4(b), radial velocities of V1363 Ori are taken from Pych et al. (2004), while our new *BVR$_c$* light curves are shown in Figure 1(b). To derive the orbital and geometric parameters, the multi-color light curves and radial velocity curves are simultaneously solved. The input mass ratio is $q = 0.205$ (Pych et al. 2004). Considering its low light variable amplitude ($\sim 0^m.20$), this might result from the existence of an undetectable companion, although searching for a tertiary component has been unsuccessful (Pribulla & Rucinski 2006; D'Angelo et al. 2006). Unfortunately, we are unable to obtain a convergent solution if the third light is a free parameter. Therefore, the final solution is listed in Table 6, in which the orbital inclination of $i = 56.9°$ is somewhat higher than the previously derived values, i.e., $54.1°$ (Gazeas et al. 2021) and $56.59°$ (Gazeas & Niarchos 2005). The fill-out factor is $f = 56.6(\pm1.5)\%$, which implies that V1363 Ori is a deep, low-mass ratio overcontact binary (Yang & Qian 2015).

5 DISCUSSIONS

5.1 Absolute Parameters and Evolutionary States

From our updated solutions, we redetermined the masses based on the mass ratio of $q = M_s/M_p$ and Kepler's third law, $(M_p + M_s) = 0.0134 \times a^3/P^2$, in which a and P are the separation between both components a, and the orbital period P. The equivalent radius is deduced from the relative radii for each component. Absolute luminosities are estimated based on a relation of $L/L_\odot = (R/R_\odot)^2(T/T_\odot)^4$, in which $R_\odot$ and $T_\odot$ are the solar radii and surface temperature. All absolute parameters for Y Sex and V1363 Ori are listed in Table 6. In fact, the standard errors of the parameters in this table are not real or formal ones, but they are computed from the W-D code (Prša & Zwitter 2005). Exploration of the parameter space with Bayesian modeling with MCMC overcomes this deficiency of W-D program and is the standard approach to modeling eclipsing binaries.

We then plotted the primary components in a temperature-luminosity diagram, which is displayed in Figure 5. In this figure, stellar evolutionary tracks are taken from (Girardi et al. 2000) for the solar chemical composition, including the zero age main sequence (ZAMS), terminal age main sequence (TAMS), evolutionary tracks, and isochrones lines. The primaries lie between the ZAMS and TAMS lines, which implies that they are slightly evolved MS stars. Based on the evolutionary track of a single star, we estimated the possible evolutionary ages to be ~ 2.51 Gyr for Y Sex and ~ 3.56 Gyr for V1363 Ori, respectively.
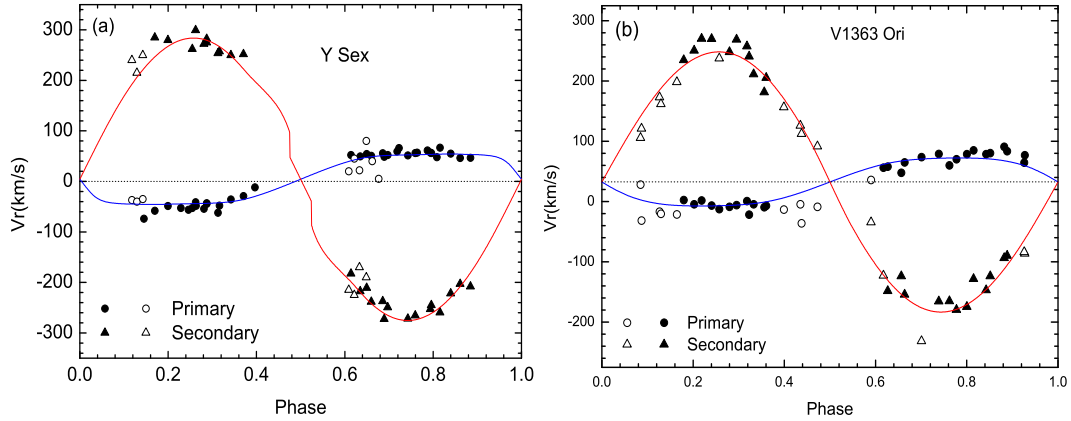
Fig. 4 (a) Radial velocities for Y Sex, in which *filled* and *open symbols* are taken from Pribulla et al. (2009) and McLean & Hilditch (1983), respectively. (b) Radial velocities of V 1363 Ori taken from Pych et al. (2004), in which *open symbols* indicate data contributing half the weight as the *solid symbols*. Theoretical RVs are plotted as *continuous color lines*, which are computed by the solutions listed in Table 6, respectively.

Table 5 All Collected Times of Minimum Light for V1363 Ori

JD(Hel.)	Error (d)	Epoch	Method	Min	$(O-C)_i$ (d)	$(O-C)_f$ (d)	Ref.
2448500.0343		−9261.0	pe	I	+0.0171	+0.0013	[1]
2452237.2413		−608.5	CCD	II	+0.0012	+0.0034	[2]
2452592.4999	±0.0020	214.0	pe	I	+0.0022	+0.0013	[3]
2452618.6316	±0.0004	274.5	pe	II	+0.0026	+0.0013	[4]
2452695.2984	±0.0008	452.0	CCD	I	+0.0028	+0.0008	[5]
2452705.2324	±0.0005	475.0	CCD	I	+0.0026	+0.0004	[5]
2452988.1425		1130.0	CCD	I	+0.0024	−0.0020	[6]
2452989.0143		1132.0	CCD	I	+0.0104	+0.0060	[6]
2452990.0946		1134.5	CCD	II	+0.0109	+0.0065	[6]
2453317.7003	±0.0003	1893.0	CCD	I	+0.0022	−0.0004	[7]
2453374.7158	±0.0001	2025.0	CCD	I	+0.0037	+0.0018	[8]
2453433.2473	±0.0010	2160.5	CCD	II	+0.0095	+0.0083	[5]
2453436.2638	±0.0012	2167.5	CCD	II	+0.0025	+0.0014	[5]
2453447.2824	±0.0007	2193.0	CCD	I	+0.0070	+0.0061	[5]
2453708.1365		2797.0	CCD	I	−0.0210	−0.0190	[9]
2454074.2131		3644.5	CCD	II	+0.0000	+0.0054	[10]
2454091.698	±0.001	3685.0	CCD	I	−0.0081	−0.0025	[11]
2454423.2007		4452.5	CCD	II	−0.0071	+0.0006	[12]
2454428.1614		4464.0	CCD	I	−0.0135	−0.0057	[12]
2454820.9961		5373.5	CCD	II	−0.0137	−0.0045	[13]
2454872.6159	±0.0001	5493.0	CCD	I	−0.0089	+0.0005	[14]
2455126.1520		6080.0	CCD	I	−0.0122	−0.0025	[15]
2455470.6205	±0.0006	6877.5	CCD	II	−0.0031	+0.0064	[16]
2455944.6503	±0.0002	7975.0	CCD	I	−0.0100	−0.0018	[17]
2456294.9455		8786.0	CCD	I	−0.0052	+0.0011	[18]
2456659.0578		9629.0	CCD	I	−0.0049	−0.0013	[19]
2456930.3163		10257.0	CCD	I	+0.0053	+0.0061	[19]
2456985.3815	±0.0015	10384.5	pe	II	+0.0002	+0.0004	[20]
2457014.1026		10451.0	CCD	I	−0.0017	−0.0017	[19]
2457425.7344	±0.0002	11404.0	CCD	I	+0.0065	+0.0011	[21]
2457448.6223	±0.0021	11457.0	CCD	I	+0.0025	−0.0033	[22]
2457725.0610		12097.0	CCD	I	+0.0098	+0.0000	[23]
2457731.9679		12113.0	CCD	I	+0.0059	−0.0040	[23]
2458871.1685	±0.0004	14750.5	CCD	II	+0.0067	+0.0000	[24]
2458872.0296	±0.0005	14752.5	CCD	II	+0.0040	−0.0028	[24]
2458902.0506	±0.0003	14822.0	CCD	I	+0.0063	−0.0004	[24]
2459244.1341	±0.0005	15614.0	CCD	I	+0.0059	+0.0001	[24]
2459244.9973	±0.0002	15616.0	CCD	I	+0.0053	−0.0006	[24]
2459246.0767	±0.0004	15618.5	CCD	II	+0.0049	−0.0010	[24]

Notes: [1] Selam (2004); [2] Kato & Takamizawa (2002); [3] Pych et al. (2004); [4] Parimucha et al. (2009); [5] Karampotsiou et al. (2016); [6] Nagai (2004); [7] Dvorak (2005); [8] Nelson (2006); [9] Nagai (2006); [10] Nagai (2007); [11] Nelson (2007); [12] Nagai (2008a); [13] Nagai (2009); [14] Dvorak (2010); [15] Nagai (2010); [16] Brát et al. (2011); [17] Nelson (2013): [18] Nagai (2014); [19] Nagai (2015); [20] Hübscher (2016); [22] Juryšek et al. (2017); [23] Nagai (2017); [24] Present paper.

Table 6 Modeling Solutions and Absolute Parameters for Two Contact Binaries

Parameters	Y Sex		V1363 Ori	
	Primary	Secondary	Primary	Secondary
$q = M_s/M_p$	0.1954($\pm$0.0009)		0.205($\pm$0.005)	
a ($R_\odot$)	2.905($\pm$0.034)		2.706($\pm$0.026)	
V_γ (km s^{-1})	4.70($\pm$1.10)		32.6($\pm$0.9)	
i ($^\circ$)	77.67($\pm$0.19)		56.9($\pm$0.2)	
$\Omega_{p,s}$	2.1579($\pm$0.0020)		2.1712($\pm$0.0020)	
T (K)	6400($\pm$100)	6211($\pm$7)	6156($\pm$76)	5627($\pm$12)
X, Y	0.646, 0.237	0.647, 0.230	0.648, 0.227	0.650, 0.200
x_B, y_B	0.809, 0.241	0.819, 0.219	0.822, 0.212	0.847, 0.127
x_V, y_V	0.719, 0.281	0.733, 0.272	0.737, 0.269	0.772, 0.217
x_{Rc}, y_{Rc}	0.647, 0.285	0.660, 0.279	0.664, 0.277	0.703, 0.241
$^a\ell_B$	0.8299($\pm$0.0069)	0.1701	0.8731($\pm$0.0021)	0.1269
ℓ_V	0.8236($\pm$0.0069)	0.1764	0.8562($\pm$0.0018)	0.1438
ℓ_{R_c}	0.8205($\pm$0.0073)	0.1795	0.8473($\pm$0.0017)	0.1527
$^b\ell_{3B}$	0.58($\pm$0.05)%		$-$	
ℓ_{3V}	0.55($\pm$0.05)%		$-$	
ℓ_{3R_c}	0.82($\pm$0.06)%		$-$	
r_{pole}	0.5042($\pm$0.0020)	0.2488($\pm$0.0012)	0.5014($\pm$0.0018)	0.2474($\pm$0.0013)
r_{side}	0.5545($\pm$0.0022)	0.2614($\pm$0.0014)	0.5505($\pm$0.0024)	0.2596($\pm$0.0017)
r_{back}	0.5819($\pm$0.0028)	0.3144($\pm$0.0020)	0.5773($\pm$0.0030)	0.3091($\pm$0.0019)
f (%)	50.8($\pm$1.6)		56.6($\pm$1.5)	
M ($M_\odot$)	1.559($\pm$0.055)	0.305($\pm$0.007)	1.181($\pm$0.034)	0.242($\pm$0.007)
R ($R_\odot$)	1.589($\pm$0.021)	0.799($\pm$0.011)	1.470($\pm$0.017)	0.736($\pm$0.009)
L ($L_\odot$)	3.794($\pm$0.100)	0.850($\pm$0.023)	2.779($\pm$0.063)	0.487($\pm$0.012)

Notes: ^{a,b}The relative luminosities can be expressed by $\ell_{p/s} = L_{p/s}/(L_p + L_s)$ and $\ell_3 = L_3/(L_p + L_s + L_3)$ for BVR bands, respectively.
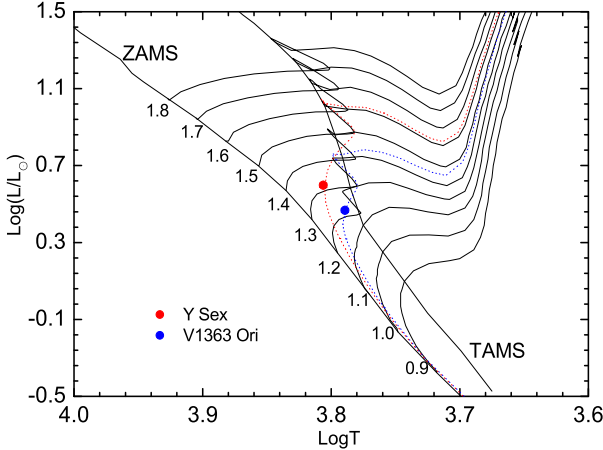

Fig. 5 Primary components for Y Sex and V1363 Ori in the H-R diagram. Evolutionary tracks for stellar mass from 0.9 $M_\odot$ to 1.8 $M_\odot$ with solar chemical compositions taken from Girardi et al. (2000). The *dotted color lines* are isochrone lines.

5.2 Magnetic Activity Cycles or the Third Body?

For Y Sex and V1363 Ori, there evidently exist quasi-cyclic variations from their $(O - C)$ curves of Figure 3. This case occurs in other DLMR overcontact binaries Yang & Qian (2015), such as CK Boo (Yang 2012), V345 Gem (Yang 2009) and AH Cnc (Peng et al. 2016). For the late-type contact binaries, their cyclic oscillations may generally result from magnetic activity cycles (Applegate 1999) or light-time effect via the presence of the third body (Irwin 1952). Applegate (1999) suggested that the gravitational coupling mechanism causes the

cyclic magnetic activity, which may produce the observed amplitude of period modulation. We then compute the value of $\Delta P/P$ with the help of the following equation,

$$\frac{\Delta P}{P} = A \times \sqrt{2[1 - \cos(\frac{2\pi P}{P_{mod}})]} \simeq \frac{2\pi A}{P_{mod}}, \quad (4)$$

in which A is $a_{12}\sin i/c$. The calculated values for two contact binaries approximate to the typical value of $\Delta P/P \sim 10^{-5}$. For V1363 Ori, the O'Connell effect occurs in previous light curves (Gomez-Forrellad et al. 1999; Gazeas & Niarchos 2005). So we could not remove the magnetic activity mechanism.

Alternatively, this kind of oscillations may result from the light-time effect via by the presence of the third body. (Irwin 1952). Its mass function is computed by the known equation,

$$f(m) = \frac{4\pi^2}{GP_3^2} \times (a_{12}\sin i)^3 = \frac{(M_3\sin i)^3}{(M_1 + M_2 + M_3)^2}. \quad (5)$$

By the iteration method for Equation (5), we can compute the minimum mass M_3 and a_{12} for the orbital inclination $i = 90^\circ$, which are listed in Table 4. According to Allen's table (Cox 2000), we can estimate the spectral types of K7 for Y Sex and M4 for V1363 Ori, respectively. The angular separation of the third body from the binary α can be estimated from the parallaxes (Gaia Collaboration et al. 2018). Therefore, it is difficult to identify the third bodies due to the low luminosity and small angular separation.

Table 7 Several Low-mass Ratio Contact Binaries with Secular Period Increasing

Star	Sp.	Period (d)	Type	q	M_p $(M_\odot)$	f (%)	dP/dt $(\times 10^{-7}\mathrm{d\ yr^{-1}})$	Reference
XY Boo	F5V	0.37055	A	0.186	0.912	55.9	1.44	Özavci et al. (2020)
V1191 Cyg	F6V	0.31338	W	0.107	1.31	68.6	4.50	Zhu et al. (2011)
V345 Gem	F7V	0.27477	W	0.142	1.05	73.3	0.59	Yang (2009)
V1363 Ori	F6	0.43192	A	0.205	1.181	56.5	1.56	Present paper
DZ Psc	F7V	0.36613	A	0.136	1.37	79.0	7.41	Yang et al. (2013)
Y Sex	F5/6	0.41982	A	0.195	1.559	50.8	4.58	Present paper
UY UMa	G1V	0.37602	W	0.21	1.117	61	2.55	Kim et al. (2019)
CK Boo	F7/8V	0.35515	A	0.111	1.386	65.0	0.98	Yang et al. (2012)
AH Cnc	F7V	0.36048	A	0.168	1.10	51	3.99	Peng et al. (2016)
TY Pup	F2V	0.81923	A	0.184	1.650	84.3	+0.56	Sarotsakulchai et al. (2018)
II UMa	F5III	0.82522	A	0.172	1.99	86.6	+4.88	Zhou et al. (2016)
V409 Hya	F2V	0.47226	A	0.216	1.5	60.6	+5.41	Na et al. (2014)
V728 Her	F3	0.44625	A	0.158	1.8	81.0	+1.92	Erkan & Ulaş (2016)

5.3 Long-term Period Increasing

From Table 4, the orbital periods may be increasing at the rates of $dP/dt = +0.46(\pm0.04) \times 10^{-7}\mathrm{d\ yr^{-1}}$ for Y Sex and $dP/dt = +1.56(\pm0.06) \times 10^{-7}\mathrm{d\ yr^{-1}}$ for V1363 Ori, respectively. In the case of the conserved mass transfer, this kind of secular period increase may be attributed to mass transfer from the less massive component to the more massive one. By the following equation (Singh & Chaubey 1986),

$$\frac{\dot{P}}{P} = \frac{3(1-q)}{q}\frac{\dot{M}_p}{M_p},\qquad(6)$$

we can compute the mass transferring rates, i.e., $\dot{M}_p = 1.38(\pm0.10)\ \mathrm{M}_\odot\ \mathrm{yr^{-1}}$ for Y Sex and $\dot{M}_p = 3.67(\pm0.11)\ \mathrm{M}_\odot\ \mathrm{yr^{-1}}$ for V1363 Ori. This kind of secular period increasing also occurs in other DLMR overcontact binaries, which are listed in Table 7. With the period increasing, the mass transfers from the less massive component to the more massive one, which results in the mass ratio decreasing and J_{spin}/J_{orb} will increase. Meanwhile, the separation between two components increasing causes the contact degree to decrease. Only if the contact configuration does not break down, this kind of DLMR overcontact binaries, such as Y Sex and V1363 Ori, will evolve into the rapid-rotating single stars at $J_{orb} < 3J_{spin}$ (Hut 1980).

References

Agerer, F., Dahm, M., & Hübscher, J. 1999, Inf. Bull. Var. Stars, 4712, 1

Agerer, F., & Hübscher, J. 1998a, Inf. Bull. Var. Stars, 4562, 1

Agerer, F., & Hübscher, J. 1998b, Inf. Bull. Var. Stars, 4606, 1

Agerer, F., & Hübscher, J. 2002, Inf. Bull. Var. Stars, 5296, 1

Applegate, J. H. 1992, ApJ, 385, 621

Braune, W., & Hübscher, J. 1987, Berliner Arbeitsgemeinschaft fuer Veraenderliche Sterne - Mitteilungen, 46

Brát, L., Šmelcer, L., Lehký, M., et al. 2011, Open Eur. J. Var. Stars, 137, 1

Brát, L., Zejda, M., & Svoboda, P. 2007, Open Eur. J. Var. Stars, 34, 1

Cox, A. N. (ed.) 2000, Allen's Astrophisical Quantities (4th edn.) (New York: Springer)

Csizmadia, S., & Klagyivik, P. 2004, A&A, 426, 1001

Dai, H.-F., Yang, Y.-G., & Yin, X.-G. 2011, New Astron., 16, 173

D'Angelo, C., van Kerkwijk, M. H., & Rucinski, S. M. 2006, AJ, 132, 650

Diethelm, R. 1998, BBSAG Bull., 108, 8

Diethelm, R. 2001, BBSAG Bull., 125, 7

Diethelm, R. 2009, Inf. Bull. Var. Stars, 5894, 1

Diethlem, R. 2010, Inf. Bull. Var. Stars, 5945, 1

Diethlem, R. 2011, Inf. Bull. Var. Stars, 5992, 1

Diethlem, R. 2012, Inf. Bull. Var. Stars, 6029, 1

Dvorak, S. W. 2005, Inf. Bull. Var. Stars, 5603, 1

Dvorak, S. W. 2010, Inf. Bull. Var. Stars, 5938, 1

ESA, 1997, The *Hipparcos* and *Tycho* Catalogs, (ESA SP 1200; Noordwijk: ESA)

Eggleton, P. P. 2000, New Astron. Rev., 44, 111

Eggleton, P. P. 2006, Evolutionary Process in Binary and Multiple Systems (Cambridge: Cambridge Univ. Press)

Erkan, N., & Ulaş, B. 2016, New Astron., 46, 73

Flannery, B. P. 1976, ApJ, 205, 217

Gaia Collaboration, Brown, A. G. A., Vallenari, A., et al. 2018, A&A, 616, 1

Gazeas, K. D., Zola, S., Liakos, A., et al. 2021, MNRAS, 501, 2897

Gazeas, K. D., & Niarchos, P. 2005, Aerosp. Res. Bulgaria, 20, 193

Geske, M., Gettel, S. J., & McKay, T. A. 2006, AJ, 131, 633

Girardi, L., Bressan, A., Bertelli, G., & Chiosi, C. 2000, A&AS, 141, 371

Gomez-Forrellad, J. M., Garsia-Melendo, E., Guarro-Flo, J., et al. 1999, Inf. Bull. Var. Stars, 4702, 1

Gu, Shenghong 1998, Publications of the Yunnan Observatory, 1, 7

He, J.-J., & Qian, S.-B. 2007, PASJ, 59, 1115

Herczeg, T. J. 1993, PASP, 105, 911

Hill, G. 1979, Publ. Dom. Astrophys. Obs., 15, 297

Hoffmeister 1934, Astron. Nachr., 253, 195

Huruhata 1958, DLich ATOK, 5, 3

Hut, P. 1980, A&A, 92, 167

Hübscher, J. 2005, Inf. Bull. Var. Stars, 5643, 1

Hübscher, J. 2007, Inf. Bull. Var. Stars, 5802, 1

Hübscher, J. 2013, Inf. Bull. Var. Stars, 6084, 1

Hübscher, J. 2016, Inf. Bull. Var. Stars, 6157, 1

Hübscher, J. 2017, Inf. Bull. Var. Stars, 6196, 1

Hübscher, J., Agerer, F., Frank, P., & Wunder, E. 1994, Berliner Arbeitsgemeinschaft fuer Veraenderliche Sterne - Mitteilungen, 68, 1

Hübscher, J., Agerer, F., & Wunder, E. 1991, Berliner Arbeitsgemeinschaft fuer Veraenderliche Sterne - Mitteilungen, 59, 1

Hübscher, J., Agerer, F., & Wunder, E. 1992, Berliner Arbeitsgemeinschaft fuer Veraenderliche Sterne - Mitteilungen, 60, 1

Hübscher, J., Agerer, F., & Wunder, E. Berliner Arbeitsgemeinschaft fuer Veraenderliche Sterne - Mitteilungen, 1993, 62, 1

Hübscher, J., & Lehmann, P. B. 2015, Inf. Bull. Var. Stars, 6149, 1

Hübscher, J., & Lichtenknecker, D. 1988, Berliner Arbeitsgemeinschaft fuer Veraenderliche Sterne - Mitteilungen, 50

Hübscher, J., Lichtenknecker, D., & Mundry, E. 1985, BAV Mitt., 39, 4

Hübscher, J., Lichtenknecker, D., & Wunder, E. 1989, Berliner Arbeitsgemeinschaft fuer Veraenderliche Sterne - Mitteilungen, 52

Hübscher, J., & Monninger, G. 2011, Inf. Bull. Var. Stars, 5959, 1

Hübscher, J., Paschke, A., & Walter, F. 2005, Inf. Bull. Var. Stars, 5657, 1

Irwin, J. B. 1952, ApJ, 116, 211

Jiang, D. 2020, MNRAS, 492, 2731

Jiang, D., Han, Z., & Li, L. 2014, MNRAS, 438, 859

Juryšek, J., Hoňková, K., Šmelcer, L., et al. 2017, Open Eur. J. Var. Stars, 179, 1

Karampotsiou, E., Gazeas, K., Petropoulou, M., & Tzouganatos, L. 2016, Inf. Bull. Var. Stars, 6158, 1

Kato, T., & Takamizawa, K. 2002, Var. Star Bull. of Japan, 39, 1, *http://vsolj.cetus-net.org/no39.pdf*

Kim, C.-H., Song, M.-H., Park, J.-H., et al. 2019, JASS, 36, 265

Koch, R. H. 1961, AJ, 66, 35

Kreiner, J. M. 2004, Acta Astron., 54, 207

Krajci, T. 2005, Inf. Bull. Var. Stars, 5592, 1

Krajci, T. 2006, Inf. Bull. Var. Stars, 5690, 1

Kwee, K. K., & van Woerden, H. 1956, Bull. Astron. Ins, Nerth., 12, 327

Latković, O., Čeki, A., & Lazarević, S. 2021, ApJS, 254, 10

Li, H.-L., Yang Y.-G., Su, W., et al. 2009, RAA (Research in Astronomy and Astrophysics), 9, 1035

Lucy, L. B. 1967, Z. Astrophys., 65, 89

McLean, B. J., & Hilditch, R. W. 1983, MNRAS, 203, 1

Na, W.-W., Qian, S.-B., Zhang, L., et al. 2014, New Astron., 30, 105

Nagai, K. 2001, Var. Star Bull. Japan, 38, 1

Nagai, K. 2003, Var. Star Bull. Japan, 40, 1

Nagai, K. 2004, Var. Star Bull. Japan, 42, 1

Nagai, K. 2006, Var. Star Bull. Japan, 44, 1

Nagai, K. 2007, Var. Star Bull. Japan, 45, 1

Nagai, K. 2008a, Var. Star Bull. Japan, 46, 1

Nagai, K. 2008b, Var. Star Bull. Japan, 47, 1

Nagai, K. 2009, Var. Star Bull. Japan, 48, 1

Nagai, K. 2010, Var. Star Bull. Japan, 50, 1

Nagai, K. 2012, Var. Star Bull. Japan, 53, 1

Nagai, K. 2014, Var. Star Bull. Japan, 56, 1

Nagai, K. 2015, Var. Star Bull. Japan, 59, 1

Nagai, K. 2016, Var. Star Bull. Japan, 61, 1

Nagai, K. 2017, Var. Star Bull. Japan, 63, 1

Nagai, K. 2018, Var. Star Bull. Japan, 64, 1

Nelson, R. H. 2006, Inf. Bull. Var. Stars, 5672, 1

Nelson, R. H. 2007, Inf. Bull. Var. Stars, 5760, 1

Nelson, R. H. 2013, Inf. Bull. Var. Stars, 6050, 1

Nelson, C. A., & Eggleton, P. P. 2001, ApJ, 552, 664

Nesterov, V. V., Kuzmin, A. V., Ashimbaeva, N. T., et al. 1995, A&AS, 110, 367

Ogłoza, W., Niewiadomski, W., Barnacka, A., et al. 2008, Inf. Bull. Var. Stars, 5843, 1

Özavci, I., Özuyar, D., Şenavci, H. V., et al. 2020, Acta Astron., 70, 33

Pagel, L. 2018, Inf. Bull. Var. Stars, 6244, 1

Pagel, L. 2020, BAV Mitt., 33, 1, *https://www.bav-astro.eu/images/Up_Journal/BAVJ033_BAVM251_R1.pdf*

Parimucha, Š., Dubovský, P., Baluďanský, D., et al. 2009, Inf. Bull. Var. Stars, 5898, 1

Parimucha, Š., Dubovský, P., Vaňko, M., et al. 2011, Inf. Bull. Var. Stars, 5980, 1

Parimucha, Š., Dubovský, P., Vaňko, M., et al. 2013, Inf. Bull. Var. Stars, 6044, 1

Paschke, A. 2017, Open Eur. J. Var. Stars, 181, 1

Paschke, A. 2020, BAV Mitt., 40, 1, *https://www.bav-astro.eu/images/Up_Journal/BAVJ040_*

2_.pdf

Peng, Y.-J., Luo, Z.-Q., Zhang, X.-B., et al. 2016, RAA (Research in Astronomy and Astrophysics), 16, 157

Pribulla, T., & Rucinski, S. M. 2006, AJ, 131, 2986

Pribulla, T., Rucinski, S. M., Blake, R. M., et al. 2009, AJ, 137, 3655

Prikhodjko, A. 1947, Variable Stars (USSR), 6, 136

Prša, A., & Zwitter, T. 2005, ApJ, 628, 426

Pych, W., Rucinski, S. M., DeBond, H., et al. 2004, AJ, 127, 1712

Qian, S.-B., & Liu, Q.-Y. 2000, A&A, 355, 171

Qian, S.-B., Zhu, L.-Y., Liu, L., et al. 2020, RAA (Research in Astronomy and Astrophysics), 20, 163

Robertson, J. A., & Eggleton, P. P. 1977, MNRAS, 179, 359

Rucinski, S. M. 1973, Acta Astron., 23, 79

Samolyk, G. 2012, JAAVSO, 40, 975

Samolyk, G. 2015, JAAVSO, 43, 77

Samolyk, G. 2017, JAAVSO, 45, 215

Samolyk, G. 2018, JAAVSO, 46, 184

Samolyk, G. 2019, JAAVSO, 47, 265

Sarotsakulchai, T., Qian, S.-B., Soonthornthum, B., et al. 2018, AJ, 156, 199

Šarounová, L. & Wolf, M. 2005, Inf. Bull. Var. Stars, 5594, 1

Selam, S. O. 2004, A&A, 416, 1097

Singh, M., & Chaubey, U. S. 1986, Ap&SS, 124, 389

Sobotka, P. 2007, Inf. Bull. Var. Stars, 5809, 1

Stępień, K. 2006, Acta, Astron., 56, 199

Sun, W., Chen, X., Deng, L., & de Girijs, R. 2020, ApJS, 247, 50

Szafraniec, R. 1962, Acta Astron., 12, 181

Tanabe, H., & Nakamura, T. 1957, Ann. Tokyo Astron. Obs. 2nd Ser., 5, 1

Torres, G., Andersen, J., & Giménez, A. 2010, A&A Rev., 18, 67

Tylenda, R., Hajduk, M., Kamiński, T., et al. 2011, A&A, 528, 114

Van Hamme, W. 1993, AJ, 106, 2096

Van Hamme, W., & Cohen, R. E. 2008, The closest of the close: observational and modeling progress, in Astrophysics and Space Science Library, eds. Milone, E. F. et al. (New York: Springer)

Wadhwa, S. S., de Horta, A., Filipović, M. D., et al. 2021, MNRAS, 501, 229

Webbink, R. F. 1976, ApJ, 209, 829

Webbink, R. F. 2003, ASPC, 293, 76

Wolf, M., Molík, P., Hornoch, K., & Šarounová, L. 2000, A&AS, 147, 243

Wilson, R. E. 2008, ApJ, 672, 575

Wilson, R. E., & Devinney, E. J. 1971, ApJ, 166, 605

Wilson, R. E., Devinney, E. J., & Van Hamme, W. 2020a, Astrophysics Source Code Library, 2020ascl.soft04004W

Wilson, R. E., & Van Hamme 2014, ApJ, 780, 151

Wilson, R. E., Van Hamme, W., & Peters, G. J. 2020b, Contrib. Astron. Obs. Skalnaté Pleso, 50, 552

Yang, Yulan, & Liu, Qingyao 1982, Inf. Bull Var. Stars, 2202, 1

Yang, Yulan, & Liu, Qingyao 2003, New Astron., 8, 465

Yang, Y.-G. 2009, Science in China Series G-Physics, Mechanics & Astronomy, 39, 637 (in Chinese)

Yang, Y.-G. 2012, RAA (Research in Astronomy and Astrophysics), 12, 419

Yang, Y.-G., & Qian, S.-B. 2015, AJ, 150, 69

Yang, Y.-G., Qian, S.-B., & Soonthornthum, B. 2012, AJ, 143, 122

Yang, Y.-G., Qian, S.-B., Zhang, L.-Y., et al. 2013, AJ, 146, 35

Zejda, M. 2004, Inf. Bull. Var. Stars, 5583, 1

Zessewitsch, V. P. 1947, Dlich AC, 13, 7

Zhang, X.-D., & Qian, S.-B. 2020, MNRAS, 497, 3493

Zhang, X.-D., Qian, S.-B., & Liao, W.-P. 2020, MNRAS, 493, 4112

Zhou, X., Qian, S.-B., Zhang, J., et al. 2016, AJ, 151, 67

Zhu, L.-Y., Qian, S.-B., Soonthornthum, B., et al. 2011, AJ, 142, 124